

# SUBPICOSECOND ELECTRON BUNCH TRAIN PRODUCTION USING A PHASE-SPACE EXCHANGE TECHNIQUE \*

Y.-E. Sun<sup>1</sup>, P. Piot<sup>1,2</sup>, A. S. Johnson<sup>1</sup>, A. H. Lumpkin<sup>1</sup>, T. J. Maxwell<sup>1,2</sup>,  
J. Ruan<sup>1</sup>, and R. M. Thurman-Keup<sup>1</sup>

<sup>1</sup> Fermi National Accelerator Laboratory, Batavia, IL 60510, USA

<sup>2</sup> Department of Physics, Northern Illinois University DeKalb, IL 60115, USA

## Abstract

Our recent experimental demonstration of a photoinjector electron bunch train with sub-picosecond structures is reported in this paper. The experiment is accomplished by converting an initially horizontal beam intensity modulation into a longitudinal phase space modulation, via a beamline capable of exchanging phase-space coordinates between the horizontal and longitudinal degrees of freedom. The initial transverse modulation is produced by intercepting the beam with a multislit mask prior to the exchange. We also compare our experimental results with numerical simulations.

## INTRODUCTION

The qualities of high-brightness photoinjector electron beams are often valued in a root-mean-square (rms) sense, such as beam emittance, bunch length etc.. However, recent applications demand for more precisely tailored beam such as beams of certain temporal shape. In particular, electron bunch trains with sub-picosecond structures are desired by applications ranging from the generation of super-radiant radiation [1, 2, 3] to the resonant excitation of wakefields in novel beam-driven acceleration methods [4, 5]. To date there are very few reliable methods to produce such bunch trains [6]. Our method consists of modulating beam transverse intensity using a multi-slit mask, then exchanging the transverse and longitudinal phase space of the beam, and finally recovering the modulation in time and energy profile [7]. The phase space exchange beamline is composed of one dipole-mode RF cavity flanked by two identical doglegs, each dogleg formed by two dipole magnets (henceforth referred to as the double-dogleg beamline). Under the thin lens approximation, under phase space exchange conditions [8], the beam phase space final horizontal coordinates  $(z, \delta)$  are related to the initial horizontal coordinates  $(x_0, x'_0)$  via

$$z = -\alpha x_0 - \alpha S x'_0, \delta = -\frac{1}{\alpha L} x_0 - \frac{L+S}{\alpha L} x'_0, \quad (1)$$

where  $\alpha$  is the bending angle of the dipole magnets,  $L$  is the drift space between the dipoles in a dogleg, and  $S$  is the drift space between the middle dipole magnets and the dipole-mode cavity [9]. The coupling described by Eq. (1)

can be used to arbitrarily shape the temporal distribution of an electron beam [10].

## BEAMLINE SETUP

The experiment is carried out at the A0 photoinjector of Fermilab. The electrons are generated via photoemission from a cesium telluride photocathode located on the back plate of a 1.5-cell, 1.3 GHz RF gun. Three solenoids surrounding the RF Gun provide the transverse beam focusing and emittance control. The beam is then accelerated by a 9-cell, 1.3 GHz superconducting (SC) RF cavity to about 14 MeV. The transverse intensity shaping masks can be inserted at a location downstream of the SC RF cavity. The beam can be directed either straight ahead for transverse and longitudinal beam parameter diagnostics ("straight-ahead" beamline), or to the double-dogleg beamline for phase-space exchange between horizontal and longitudinal degrees of freedom [11]. Beam properties after phase-space exchange can also be measured by several diagnostics stations following the double-dogleg beamline; see Fig. 1. Each dipole magnet bends the beam by  $\alpha = 22.5^\circ$  and each dogleg generates a horizontal offset of 33 cm from the straight-ahead beamline;  $L = 803$  mm, and  $S = 764$  mm for A0. The spectrometer dipole bends the beam horizontally in the straight-ahead beamline and vertically in the double-dogleg beamline.

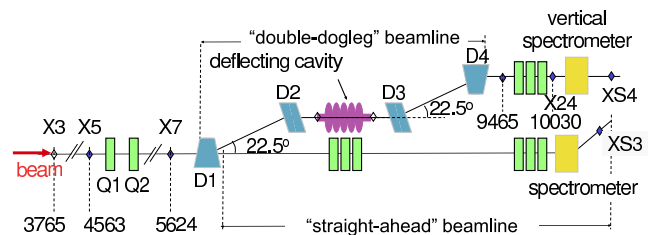


Figure 1: Top view of the 14 MeV beamlines at A0 photoinjector. The "X" refers to diagnostic stations, "Q" the quadrupole magnets and "D" the dipole magnets. Distances shown are referenced to the photocathode and in the unit of mm.

## EXPERIMENTAL RESULTS

The horizontal beam density modulation is introduced at X3 (see Fig. 1). At this location, a tungsten vertical multi-slit plate of 3 mm thickness can be inserted. The slits are

\* The work was supported by the Fermi Research Alliance, LLC under the DOE Contract No. DE-AC02-07CH11359, and by Northern Illinois University under the DOE Contract No. DE-FG02-08ER41532.

48  $\mu\text{m}$  wide and separated by 1 mm. Two quadrupoles (Q1 and Q2) are available upstream of the double-dogleg beam-line for the fine tuning of the transverse Courant-Snyder parameters. This provides the control of the bunch train temporal structure downstream of the double-dogleg beamline.

The temporal characteristics of the electron beam are diagnosed using the coherent transition radiation (CTR) generated as the beam impinges an aluminium screen inserted at X24. The CTR signal transmitted through a single-crystal quartz window is sent to a Michelson autocorrelator [12]. The autocorrelation function is measured by a liquid helium-cooled bolometer used as the detector of the autocorrelator. A photo of the experimental setup and schematics is shown in Fig. 2.

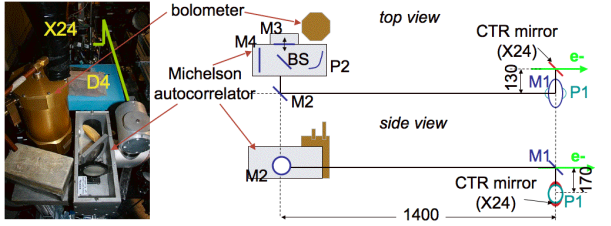


Figure 2: Beam temporal diagnostics: Michelson autocorrelator and its detector which is a liquid-helium-cooled bolometer.

Within the detector bandwidth, the signal measured by the bolometer is inversely proportional to the rms bunch length [13]. The currents of quadrupoles Q1 and Q2 are scanned while the bolometer signal is recorded. Such a quadrupole scan map provides proper tuning of the initial beam transverse properties before the phase-space exchange. A comparison with the vertical multislit at X3 in/out the beamline is shown in Fig. 3. While the major banana-shaped island provides the working points for an overall compressed beam, the smaller island which appeared on the lower right corner when the X3 slits are inserted is related to the coherent radiation produced by the bunch-train structure of the electron beam. The five white dots in Fig. 3 indicate the quadrupole settings at which we took detailed measurements of the beam longitudinal properties.

Keeping the current of quadrupole Q2 fixed at -0.6 A, we scan the current of Q1 from 1.0 A to 1.8 A. The autocorrelation functions measured by the bolometer are shown in Fig.4. The 100% modulation of the autocorrelation function implies that the bunches within the train are completely separated.

The bunch train separation is extracted from the measured autocorrelation function. The minimum measured separation is 350  $\mu\text{m}$ . Assuming the bunches are Gaussian longitudinally, the estimated rms bunch length is less than 300 fs (which includes the 200 fs resolution of our measurement system). The separation is almost doubled as  $I_{Q1}$  increased from 1.0 A to 1.8 A which is a relatively wide

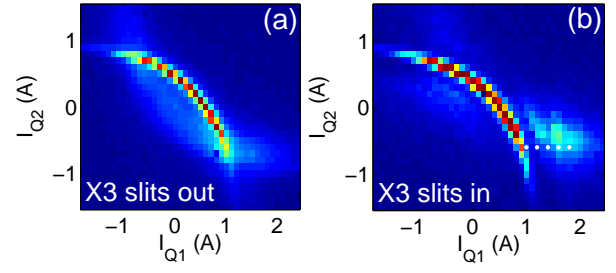


Figure 3: Total normalized CTR energy detected at X24 as a function of quadrupole magnets currents  $I_{Q1}$  and  $I_{Q2}$  with X3 slits out(a) and in (b) the beamline. The bolometer signal is representative of the inverse of the bunch duration  $\sigma_t$ .

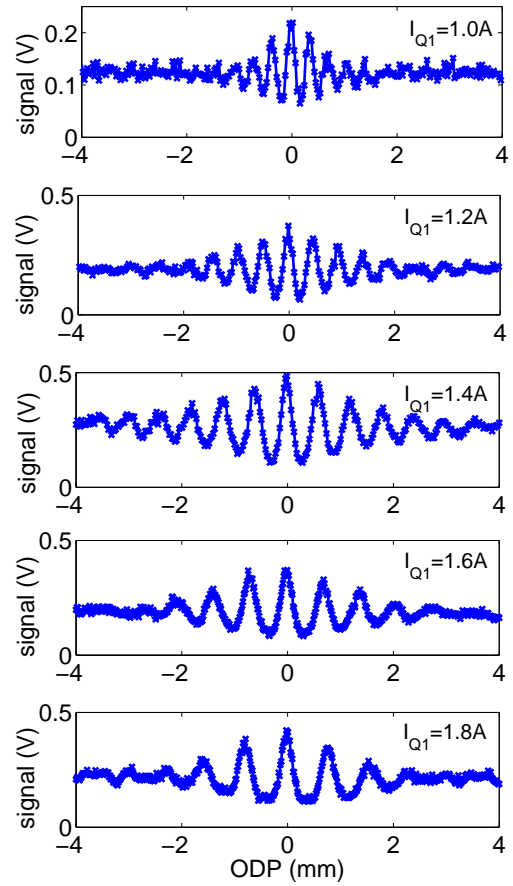


Figure 4: Autocorrelation signal from the bolometer as the current of quadrupole Q1 is varied from 1.0A to 1.8 A. The current of quadrupole Q2 is fixed at -0.6A.

range, see Fig. 5.

As seen from Eq. (1), both the final longitudinal position and energy of beam is encoded with the initial transverse position information. Therefore we expect a similar energy modulation as in the beam's temporal profile. Indeed, beam energy modulation is observed on the spectrometer screen at XS4 at the same machine settings. In Fig. 6, a series of

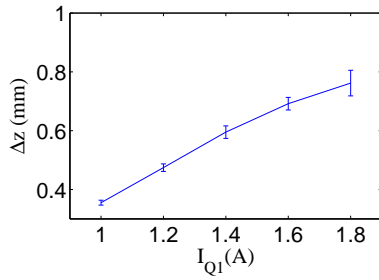


Figure 5: Bunch train separation as a function of the current of quadrupole Q1. The current of quadrupole Q2 is fixed at -0.6A.

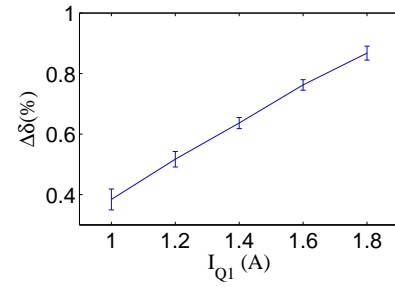


Figure 7: Fractional momentum spread separation as a function of the current of quadrupole Q1. The current of quadrupole Q2 is fixed at -0.6A.

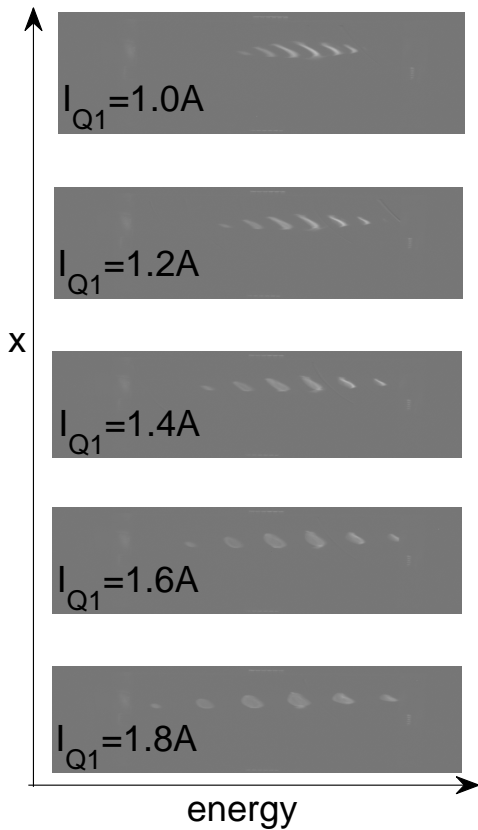


Figure 6: The energy of the bunch train as the shown on the XS4 spectrometer screen; the current of quadrupole Q1 is varied from 1.0A to 1.8 A.  $I_{Q2}$  is fixed at -0.6A.

images are taken when  $I_{Q1}$  is varied from 1.0 A to 1.8 A.

The fractional momentum spread separation between the bunches in the train is extracted from spectrometer images; the results are plotted in Fig. 7. Compared with Fig. 5 we can see the strong correlation in the two coordinates of the longitudinal phase space.

## SUMMARY

We have demonstrated experimentally the generation of a sub-ps bunch train using the phase-space exchange method. The time structure can be easily controlled by tuning the initial beam's horizontal Courant-Snyder parameters using a couple of quadrupole magnets. Further improvement of the experiment is underway. We have recently replaced the single-crystal quartz vacuum window at X24 with a diamond window, this will allow the shorter wavelength CTR signal (up to a couple of tenths of  $1 \mu\text{m}$ ) to be transferred to the bolometer; the quartz window has a transmission cut-off of around  $100 \mu\text{m}$ . We are considering using an optimized multislit plate at X3 (the one we have used is designed for beam emittance measurement), for either shorter or variable bunch separation purposes.

We thank our colleagues E. Harms, E. Lopez, R. Montiel, W. Muranyi, J. Santucci, C. Tan and B. Tennis for their technical supports, M. Church, H. Edwards, and V. Shiltsev for their interest and encouragement.

## REFERENCES

- [1] A. Gover, *Phys. Rev. ST Accel. Beams* **8**, 030701 (2005).
- [2] M. Bolosco, *et al.*, *Nucl. Instr. Meth. A* **577**, 409 (2007).
- [3] Y.-C. Huang, *Int. Jour. Mod. Phys. B* **21**, 287 (2007).
- [4] P. Muggli, *et al.*, *Phys. Rev. ST Accel. Beams* **13**, 052803 (2010).
- [5] C. Jing *et al.*, *Phys. Rev. Lett.* **98**, 144801 (2007).
- [6] P. Muggli, *et al.*, *Phys. Rev. Lett.* **101**, 054801 (2008).
- [7] Y.-E Sun, *et al.*, *Phys. Rev. Lett.* **105**, 234801 (2010).
- [8] P. Emma, *et al.*, *Phys. Rev. ST Accel. Beams* **9**, 100702 (2006).
- [9] Y.-E Sun, and P. Piot, *Proc. LINAC08*, 498 (2009).
- [10] P. Piot, *et al.*, *Phys. Rev. ST Accel. Beams* **14**, 022801 (2011).
- [11] A. Johnson, *et al.*, *Proc. IPAC2010*, 4614, Kyoto, Japan (2010); WEP024, *Proc. of PAC11*, New York (2011).
- [12] U. Happek, *et al.*, *Phys. Rev. Lett.* **67**, 2962 (1991).
- [13] P. Piot, *et al.*, *Phys. Rev. ST Accel. Beams* **6**, 033503 (2003).